Effect of Plain and Carboxylated Styrene-Butadiene Rubber on the Rheological Behavior of Silica Fume-Class G Portland Cement Slurries

Fabrício de Campos Vitorino[a]*, Jo Dweck[b], Liberato Ferrara[c] and Romildo Dias Toledo Filho[a]

[a]Civil Engineering Program, COPPE, Universidade Federal do Rio de Janeiro, P.O. Box 68506, CEP 21941-972, Rio de Janeiro – RJ, Brazil.

[b]School of Chemistry - Federal University of Rio de Janeiro, Brazil – R. Horácio de Macedo, Cidade Universitária, Rio de Janeiro-RJ, CEP:21941-450.

[c]Department of Civil and Environmental Engineering, Politecnico di Milano, piazza Leonardo da Vinci 32, 20133 Milano, Italy

ABSTRACT

The incorporation of a high pozzolan content in cement systems enables an enhanced thermal stability. In an even harsher condition, where imposed deformations occur in addition to the high temperature, such as those found in oil wells subjected to cyclic steam stimulations, it is desirable that cementitious systems present high ductility, which can be achieved for example by adding polymers. The aim of this paper, is to better understand the rheological behavior of ductile cement slurries, designed for oil wells subjected to cyclic steam stimulation. The studied cement formulations contain Silica Fume and two different copolymers (Styrene-Butadiene, SBR and its carboxylated version, XSBR). The influence of each copolymer content on the rheological parameters was investigated. Isothermal calorimetry was used to measure the induction period to guarantee that rheological parameters were carried out in the same hydration period. As the rheometer test was carried out in a non-isothermal condition together with a vane applied shear rate, increased reaction rates are expected. However, it is plausible to assume that the pastes remained in the induction period otherwise would be in the acceleratory period where pastes start to set. Attempts have been done to correlate properties found by rheometry in mini-slump test. It was observed that the XSBR delays and decreases the ettringite formation in the first hours of cement hydration, leading to lower yield stress values and increased viscosity and thixotropy. This behavior is more pronounced for higher contents of XSBR. Good correlations were established between parameters measured by rheometry and mini-slump tests, which show promising results for potential use for on-site yield stress and plastic viscosity tests in Oil Well applications.

Keywords

Rheology; Time dependence; Styrene-Butadiene Latex; Oil well cement paste; Slump test;

1

Nomenclature and abbreviations list

$\dot{\gamma}$ – Shear rate

μ_0 – Plastic viscosity

τ – Shear stress

τ_0 – Dynamic yield stress

$c_{p,I}$ – i component specific heat

$c_{p,r}$ – Water specific heat

D_c – Cutoff spread diameter

k – Consistency index

m_i – i component mass

m_r – Water masse

n – Flow behavior index

OPC – Ordinary Portland cement

SP – Superplasticizer

STG – Static gel strength

T_c – Cutoff time of the spread velocity

TC – Time since the first water to cement contact

TT – Time since the beginning of the rheological test

1   Introduction

Oil well cementing systems must be designed to withstand challenging working scenarios, such as high temperature steam stimulation, resulting into high pressures, temperatures above 250ºC and imposed deformations due to the surrounding rock formation and the steel pipe volumetric expansion [1–3]. Pozzolanic additions, such as silica fume, have been effectively employed to face high temperature problems [3–6]. It is also seen that silica fume enhance mechanical properties [7,8]. To effectively withstand imposed deformations without undergoing disruptive damage, it is required that cement-based materials possess enhanced deformation capacity [9,10], otherwise the cemented region will fail by either cracking or debonding, leading to undesirable fluids migration and expensive remedial operations or well abandonment [1,11].

An enhanced deformation capacity can be achieved, among other options, by means of polymer addition to cement pastes, which has been addressed as a non-conventional method of enhancing the properties of cement-based materials [12,13]. Several polymer types are available in the market, with different molecular structures, which promote singular interactions with the cement medium, impacting changes in the hydration kinetics and product formation [12,14,15]. With reference to ordinary Portland cement (OPC) hydration, four main periods can be observed: pre-induction, induction, acceleration and deceleration, which occur consecutively [16–18]. The first

two occur when the material is still in the fluid state, whereas the other two occur when transition into the hardened state has already started [16,17]. Considering the aforesaid scenario, Styrene-Butadiene Rubber copolymers (SBR) are an optimal option, due to their high thermal stability (decomposition starting at 300ºC) [6]. SBR can be obtained from different chemical routes, leading to different SBR molecular structures, as well as through the addition of carboxyl groups (XSBR). This results into different properties and interactions with the cement matrix, leading to different hydration kinetics at the different cement hydration stages [18–21], which may also affect directly the rheological response of the cement paste, when in fluid state.

In fact, the rheological properties of cement pastes are likewise crucial during the slurry placement in order to guarantee the effective completion of the annulus between the steel pipe and the rock formation. Therefore, the availability of trustful rheological data is of the utmost importance to predict the successful placement of the cemented region. However, several testing protocols and standards do not take into account key factors that strongly affect rheological properties, such as boundary effects caused by the equipment geometry and strong time dependence of cement paste behavior due to hydration reactions. In relation to rheology, cement pastes can be considered as non-Newtonian fluids with a plastic component in a flow curve, and once they start flowing, after respective yield stress is attained, viscosity may increase linearly with strain rate (plastic behavior) or decrease as strain rate increases (pseudoplastic behavior), depending on the mix composition [22,23]. The Binghan model describes the former behavior while the Herschel-Bulkley model better describes the latter. Being more precise, cement pastes are suspensions, in which the solid particles, after a given resting time, experience gelification due to both attractive colloidal interactions and hydration process [1,24,25]. The energy necessary to breakdown this gel structure is the thixotropic energy [1,24,25]. A very high thixotropic energy is a concern in oil well field operations, once pumps have to be stopped eventually for site operations [1,2]. However, a moderate high thixotropic energy is required to avoid fluid loss when cementing oil wells with fractured formations [1,2,26].

In this paper the influence of SBR and XSBR in different contents (2.5, 4.4 and 5.9 mass%) on the rheology of a high-performance cement paste designed for oil wells subjected to high temperature cyclic steam injection is investigated. This is done by means of a sophisticated rheology test protocol that takes into account the time dependence of the hydration reaction of each paste. For this purpose Haak Mars III rheometer was used to access paste viscosity, static gel strength, yield stress and thixotropy. The equipment's vane layout prevents turbulent flow and the cup wall has lamellas that eliminate paste slippage. All the rheological measurements were carried out during the induction period, since at this stage the released energy fluctuation is low [18]. Therefore, an isothermal calorimeter was used to assess the hydration kinetics of the pastes. The use of calorimeter also enabled conclusions based on the different product formation that each paste undergoes due to the copolymers presence [15,27]., Correlations between mini-slump tests and rheological parameters were also obtained in this work, to enable feasible predictions of yield stress and plastic viscosity of cement pastes. The mini-slump tests use a video-camera to record time dependent spread flow properties of the cement pastes. Correlations were assessed between key rheological parameters of the cement pastes, which were compared to correlations obtained by other researchers [28–32].

2 Materials and Methods

2.1 Mix design

The employed reference cement paste (P0) was specially designed in a previous study to withstand thermal cycles in an oil well [33]. It consists of API Portland cement class G [34] supplied by Holcim - Brazil, 32m% of silica fume supplied by Camargo Corrêa de Laranjeiras - Brazil, 1.7m% naphthalene-based superplasticizer (SP) (with 40 m% of solid content and 60 m% of water) supplied by Anchortec Quartzolit – Brazil type Hormitec SP430. This superplasticizer content was the same for all the pastes to guarantee a minimal fluidity. It was defined in a previous study [35], which corroborate with results found in other studies [36]. All the contents are related to cement mass. The total water to cement plus silica fume mass ratio (w/b, water to binder ratio) was 0.50, which corresponds to a water to cement ratio (w/c) of 0.66. The physical and chemical compositions of the employed cement and silica fume are shown in Table 1.

The employed SBR and XSBR were supplied by Nitriflex – Brazil. They were used in latex state, having 34.5% and 49.4% of their mass as copolymer particles, respectively. The SBR molecule has a high styrene content (80%), pH 10.5 and density of 1.0 g·cm^{-3}. XSBR has a medium styrene content (50%), pH 8.6 and density of 1.0 g·cm^{-3}. Both copolymers were added to the reference paste P0 as cement and silica fume substitution in fractions of 2.5, 4.4 and 5.9% (referred to the copolymer mass content in latex). These fractions were chosen based on mechanical test responses in previous studies [6,37]. Hereafter, these pastes will be referred to as P2.5S, P4.4S and P5.9S for SBR modified pastes and P2.5X, P4.4X and P5.9X for XSBR modified pastes. As previously mentioned, the liquid phase of the suspensions was also considered for the total water content in the mixture, in order to keep the final w/c ratio equal to 0.66.

Table 1 – Chemical composition and physical properties of Portland cement class G and silica fume [6].

Oxides (%)	Cement	Silica fume
CaO	69.43	0.59
SiO$_2$	15.87	92.29
SO$_3$	3.87	1.76
Al$_2$O$_3$	3.17	1.17
K$_2$O	0.5	0.78
P$_2$O$_5$	-	0.88
Fe$_2$O$_3$	5.55	-
SrO	0.3	-
TiO$_2$	0.2	-
MnO	0.1	-
ZnO	0.1	-
L.O.I.	0.86	2.34
Density (g·cm^{-1})	3.3	2.4
Mean particle size (µm)	15.6	0.4
Max particle size (µm)	91.2	70.4

2.2 Mixing procedure

First, cement, silica fume, water, superplasticizer and latex were weighed separately in individual containers.

The mixing consisted first of homogenizing water and silica fume in a two-speed mixer bowl. They were mixed for two minutes at low speed at about 96 rpm and then at maximum speed of about 179 rpm, up to 20 minutes after joining the two materials. Eventually, the mixer was stopped, for not more than 2 minutes, to scrape the walls. This procedure qualitatively guarantees a good dispersion of the silica fume in water.

Then, cement, superplasticizer and, in case, copolymers were added, in this sequence, (in a shorter time interval than 5 minutes) while continuing to mix at low speed. At the end of the addition, high speed mixing was resumed until 30 minutes after the first contact between water and cement. When needed, the mixer was stopped to scrape the walls. Figure 1 shows the scheme of the employed mixing process, as described above. Previous studies using calorimeter have shown that, during the first 30 minutes pastes are in the pre-induction period [18], as it will be further shown. This period is characterized by a high intense heat flow generation, which level and time of occurrence is strongly affected by the copolymer type and content. Subsequently, the induction period starts, which is characterized by a low and steady heat flow [18] during which the paste is in fluid state. This period lasts about 40 minutes and due to its stabilized heat flow, it was considered as a reference hydration stage to compare the effects of SBR and XSBR contents on paste rheological properties. The room temperature was kept at 23 °C.
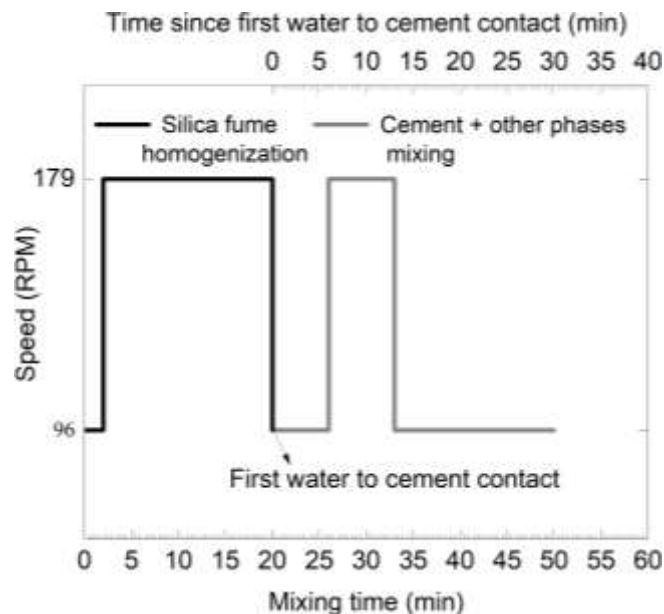

Figure 1 – Scheme of the mixing process.

2.3 Isothermal calorimetry

The effects of copolymer content on the early age hydration mechanisms of the cement pastes were studied by isothermal calorimetry in a TA Instruments, TAM air equipment. The tests were carried out at 23ºC. To avoid heating the samples, the room

temperature was 23ºC and insulating gloves were used. Glass vials filled with 2.24 g of water were used as inert reference samples in each of the eight pairs (reference/sample) of the simultaneous measurement channels of the equipment. The paste mass in the sample vials depended on its composition and it was limited to the sum of each component (i) initial heat capacity ($C_i = m_i \cdot c_{p,i}$) being equal to the heat capacity of the reference water mass ($C_r = m_r \cdot c_{p,r} = 9.36\ J \cdot K^{-1}$), according to equation 3. m_r and m_i are the water and component masses; and $c_{p,r}$ and $c_{p,i}$ are the water and component specific heats. The specific heat values adopted for each mix component are shown in Table 2.

$$m_r \cdot c_{p,r} = \sum m_i \cdot c_{p,i} \qquad \text{(Equation 3)}$$

Table 2 – Specific heat of the employed mix components.

Materials	Specific Heat	Reference
Cement (J/g·K)	0.75	[38]
Silica fume (J/g·K)	0.75	[39]
Water (J/g·K)	4.18	[38]
SBR and XSBR latex (J/g·K)	1.88	*According to the supplier*

All phases were weighed using an analytical balance with a 0.1mg resolution. The solid granular phases were weighted in plastic bags and pre-mixed manually. The liquid phases were weighted separately in syringes, after which they were added, consecutively, to the solid phase in the plastic bag and hand mixed for 1 minute keeping the bag closed. The latex was then added and the mixing continued until the composite became homogeneous for not more than 5 minutes. The time from the first contact of water with cement to the initial measurements inside the equipment varied between 5 and 12 minutes. The total lapsed time before inserting each glass vial with the respective sample inside the equipment was taken into account, for the real total analysis time. Even though all the precautions have been taken to minimize the difference between the inside and outside sample temperatures, it is worth to mention that the ideal scenario is inside equipment mixing, but due to the complex nature of the studied pastes formulation it was not feasible.

2.4 Time dependent spread tests

At the end of the mixing process, as above detailed, spread tests were carried out using a brass trunk cone, 62 mm high, having 100 and 70 mm bottom and top diameters, respectively. After mixing, the cone was placed in the upright position (smaller diameter down) over a stable and well-balanced plate. Then, the cone was completely filled with the paste under investigation. Before starting the test, a video camera with 1080 pixel/30 fps resolution, was positioned 500 mm above the trunk cone to record the test. The camera was kept recording for 1.5 minutes after the test started. ImageJ software was employed to analyze the video and to measure the evolution of the spread diameter as a function of time. As a normal human eye cannot capture and appreciate spread velocities below 0.3 mm/s, this value of the velocity was assumed

as the cutoff time of the spread velocity (T_c) [29] to identify the value of the final spread diameter, from the spread diameter vs. time evolution curves.

2.5 Rheometer tests

A Haake Mars III rheometer was used to measure the rheological behavior of the investigated reference and copolymer-modified cement pastes. The geometry of this equipment was specially designed to avoid the wall slip phenomenon and boundary effects due to low shear rates. The optical components of the equipment allow to measure shear rates in the order of 10^{-6} s^{-1}. The minimum shear stresses the equipment can measure is 10^{-6} Pa. Figure 2 shows the scheme and dimensions of the rheometer cup and vane. The tests were carried out right after the spread tests and, as the time lapsed after spread test was not significant, the same paste was recollected in a bowl container and poured into the rheometer cup until it covered the vane (Vane FL29,5). This procedure was adopted to guarantee that the same rheological properties were going to be qualitative and quantitatively measured for each of the investigated pastes through both mini-slump and rheometer tests.
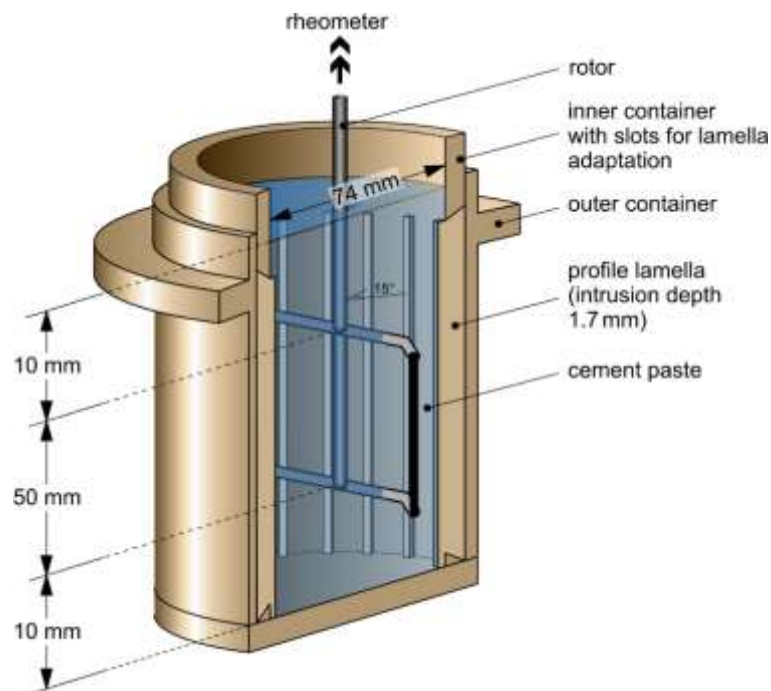

Figure 2 - Scheme of the rheometer cup with the vane used in this study.

After filling the rheometer cup, a shear rate equal to 0.1 s^{-1} was applied during the first 60 seconds to have the same shearing history for all mixtures. Next, an increasing shear ramp was applied at shear rates of 0.1, 0.3, 0.6, 3, 6, 10, 20 and 30 s^{-1}. Then, a decreasing ramp was performed using the same shear rates. Each applied shear rate lasted 10 seconds, therefore, the ramp up and down processes lasted 150 seconds as a whole. This process was repeated 4 more times after 10, 60, 300 and 600 seconds intervals, obtaining a total of 5 hysteresis curves. At this time frame all the measures were performed in the induction period. Figure 3 details rheometer test

protocol as a function of testing time and first water to cement contact time, where each peak represents a performed up and down shear ramp.
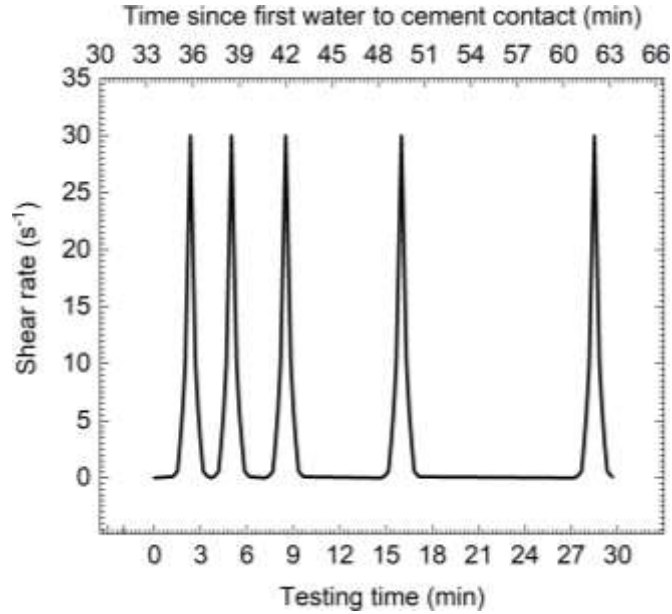

Figure 3 – Rheometer test protocol.

The static gel strength (STG), which is the stress needed to shear the paste after a resting period, was obtained at a shear rate of 0.1 s⁻¹ immediately after each resting time, at the beginning of the hysteresis loop. The Herschel-Bulkley model (equation 1) was used to identify the rheological parameters from the downward flow curves. As a matter of fact, this model provides the dynamic yield stress (τ_0), consistency index (k), shear rate ($\dot{\gamma}$) and flow behavior index (n), from which, plastic viscosity (μ_0) was calculated as shown in equation 2 [40].

Herschel-Bulkley model

$$\tau = \tau_0 + k(\dot{\gamma})^n \qquad \text{(Equation 1)}$$

Plastic viscosity expression deduced from Equation 1:

$$\mu_0 = \frac{3K}{n+2}\dot{\gamma}_{max}^{n-1} \qquad \text{(Equation 2)}$$

The thixotropy of the pastes was evaluated as proposed by Ferron *et. al.* [25]. However, adaptations had to be done to the proposed procedure, since a preliminary equilibrium loop was not performed to determine the equilibrium line in the shear stress - shear rate plot. To overcome this fact, the descending branch of the first hysteresis loop (Hysteresis 1) was taken into account as a reference line. To calculate the energy to break down the gel structure after the resting time of a given hysteresis loop, the areas between the reference line and the ascending branch of each considered hysteresis loop were calculated. In order to avoid dealing with singular points in the

8

low shear rate region, due to the elastic response of the pastes, and to reduce errors arising from that, the interval between 6 and 20 s^{-1} was taken as a reference time frame to calculate the thixotropic energy.

3   Experimental results

3.1   Hydration kinetics of SBR and XSBR cement pastes

Figure 4 shows the isothermal calorimetric curves (A and B) obtained during the pre-induction and induction periods of the reference, SBR and XSBR investigated pastes, as well as the cumulative energy released from respective hydration reactions (C and D). It is worth pointing out that during the very first minutes, where the components of the pastes were mixed outside of the calorimeter, the respective exothermic reaction effects could not be registered. In the plot one can see that, for all the three cases of SBR pastes, the maximum heat flow attained during pre-induction period was higher or at least equal to the maximum heat flow of XSBR pastes with the same copolymer content. This indicates that, considering respective mean results, during the SBR pastes pre-induction period, the ettringite ($6CaO \cdot Al_2O_3 \cdot 3SO_3 \cdot 32H_2O$) formation degree was higher than in XSBR paste cases. Even though ettringite is the dominant phase formed at this period [41], one has to consider that, despite in smaller amount, C-S-H and Portlandite are also formed during this period. This different ettringite formation can be explained by the fact that XSBR is hydrophilic, while SBR is not. Thus, the water absorption by XSBR decreases the available free water, necessary to induce the solubilization and consequent dissociation of the tricalcium aluminate ($3CaO \cdot Al_2O_3$) and gypsum ($CaO \cdot SO_3 \cdot 2H_2O$) phases, necessary to form ettringite by Eq. (3). It is also expected that XSBR carboxyl group reacts with calcium and aluminum ions forming complexes and therefore also contributing to reduce ettringite formation. XSBR complexation is discussed in more details in the topic 3.2.3.
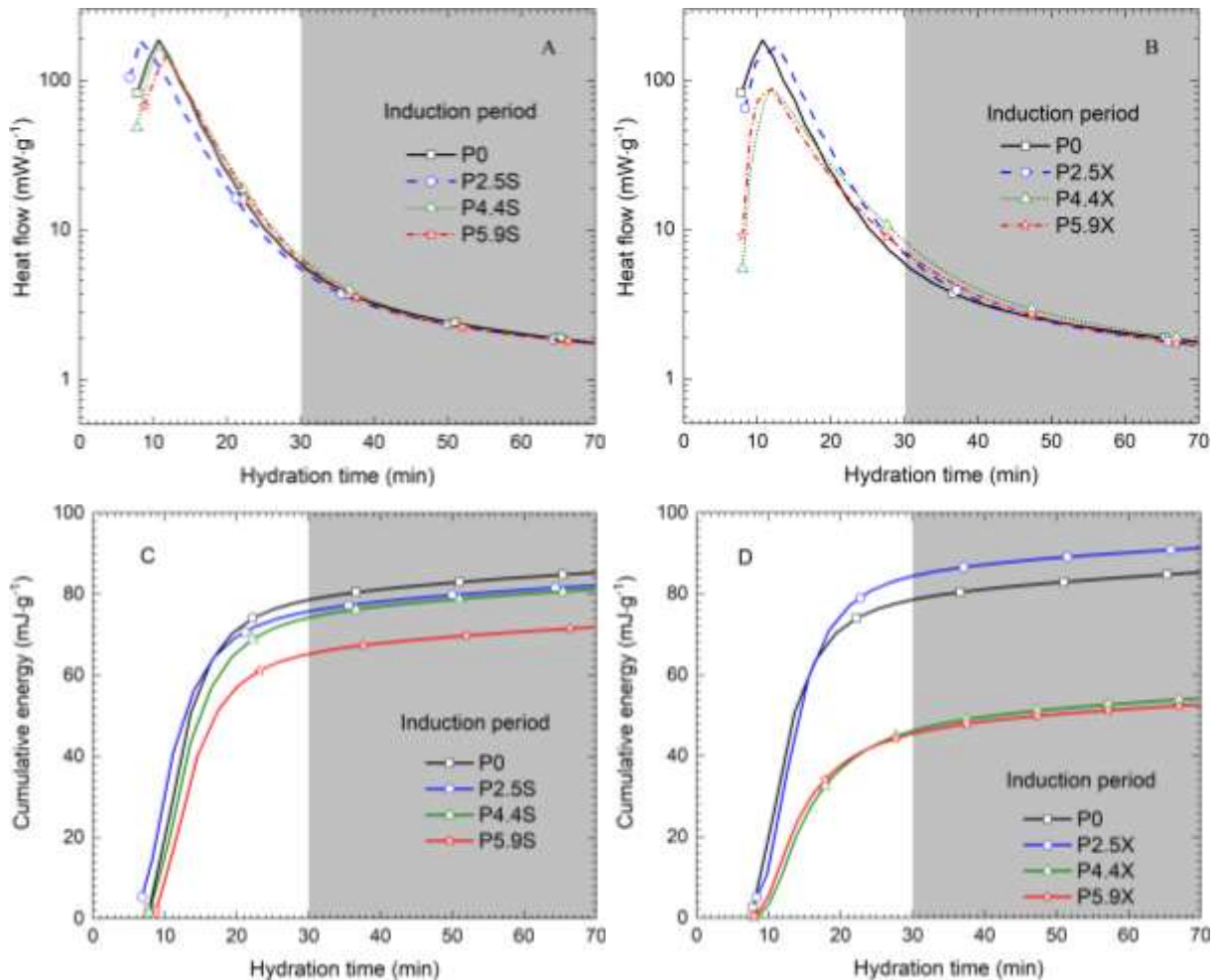
$$3CaO \cdot Al_2O_3 + 3\ CaO \cdot SO_3 \cdot 2H2O + 26\ H_2O \rightarrow 6CaO \cdot Al_2O_3 \cdot 3SO_3 \cdot 32H_2O$$
(Equation 3)
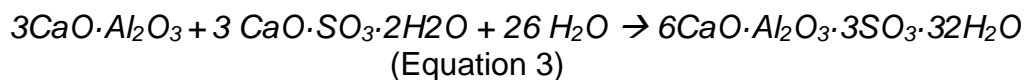
*Figure 4 – Semi-log heat flow and cartesian cumulative energy curves of pastes with different SBR contents (*A *and* C*) and different XSBR contents (*B *and* D*).*

It is worth to notice that during the ettringite formation, it precipitates as a result of its insolubility in water decreasing the remaining aqueous phase volume (which forms the remaining pores), consequently decreasing the porosity of the paste as time goes by. For the lowest XSBR content this was not verified, probably, because at this concentration, the amount of water absorbed by the polymer was not enough to decrease significantly the ettringite formation rate, which in turn occurred in the case of the two higher XSBR contents, as can be seen in Figure 4D.

Furthermore, the induction period (branched area) starts after 30 minutes of cement hydration. This represents the main value at which induction period starts (lower and maximum values equal to -2 and +8 min respectively), which does not significantly affect the results interpretation but facilitates the graphical interpretation. The starting point of the induction period of the pastes was determined by the intersection of a bilinear tangent fitting, as described in reference [18]. The heat flow generated by the hydration reactions during this period was low and decreased for each case. This indicates a reduced hydration rate, which decreases the quantity of new formed products and water consumption, which leads the composition of the present liquid and solid phases to a lower extent, resulting in minor expectable variations in the rheological properties measured during this period.

3.2 Rheometer test results

3.2.1 The flow curves

Figure 5 and Figure 6 show the shear stress vs. shear rate curves recorded at different times (time since the first water to cement contact (TC)) for pastes with different SBR and XSBR contents. Each point is a mean result of ten measurements; therefore, it is also possible to see the shear stress and shear rate standard deviation in the mean graphic. Additionally, it is possible to see a zoomed area showing the flow behavior at lower shear rates. A typical pseudoplastic behavior can be observed, together with thixotropy, from the hysteresis loops formed at different times for the pastes with different copolymer contents. It is also noticeable, in the zoomed area, that the longer the resting time, the higher is the minimum shear stress needed to yield pastes after a static period, which is the static gel strength (STG) [1,42,43]. Moreover, the increase of the copolymer content also leads to an increase in STG, as it will be highlighted in section 3.2.2.
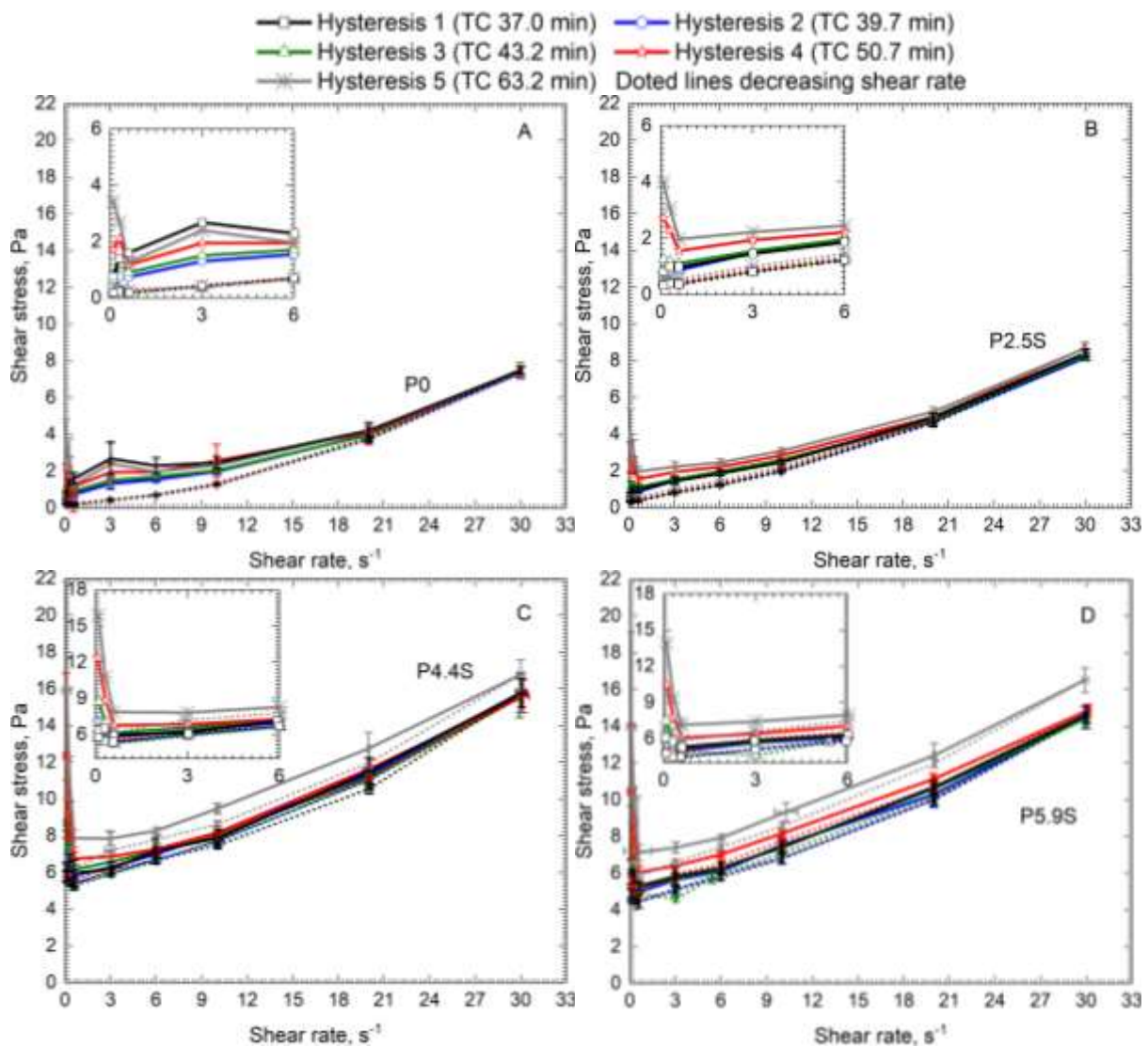

Figure 5 – Flow curves of: A – Control paste P0; B, C and D pastes with different SBR contents. TC is the time since the first water to cement contact at the end of each Hysteresis curve.
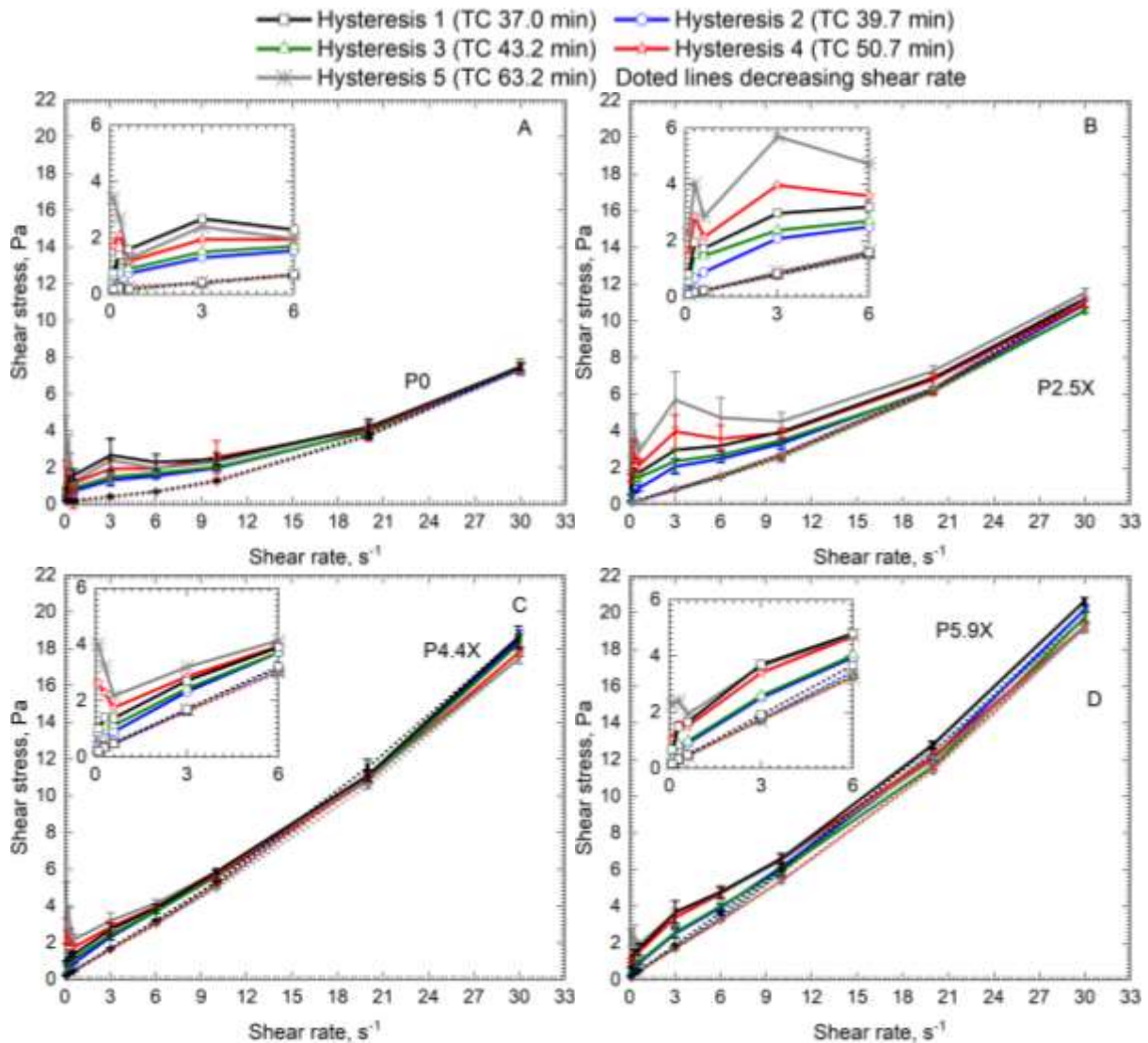
11

Figure 6 – Flow curves of: A – Control paste P0; B, C and D pastes with different XSBR contents. TC is the time since the first water to cement contact at the end of each Hysteresis curve.

3.2.2 Influence of time, copolymer type and copolymer content on the yield stress and static gel strength

The static gel strength of the pastes, measured at the beginning of each upward ramps branch of the hysteresis loop, are shown in Figure 7, where it is possible to notice the influence of each copolymer type and content along the time since the first water to cement contact (TC) and testing time (TT). TT refers to the time since the rheological test started. At a first sight, it is evident that SBR considerably affects STG, mainly for higher contents, whilst XSBR presence has minor effect on this parameter. The mid-level SBR content featured the highest STG increase and above it, slight reductions were found. Compared to the STG measured after 26 minutes for the reference paste, P4.4S paste STG increased 4.6 times, while P4.4X paste reached a maximum of 17% variation.

It is also evident that the STG is strongly affected by the resting time between the measurements. For instance, after 26 minutes, the reference paste shows 4.5 times increase with respect to the value at time 0, whilst the STG of the pastes with mid-level contents of SBR and XSBR increased 2.4 and 4.0 times, respectively, always referred to the relative value at time 0. However, it is important to notice that the pastes with the two highest contents of SBR found STG absolute values much higher than those of the reference paste, while for XSBR pastes, the STG values were of the same order as of those found for reference paste, except for P5.9X paste which presented slight lower values.
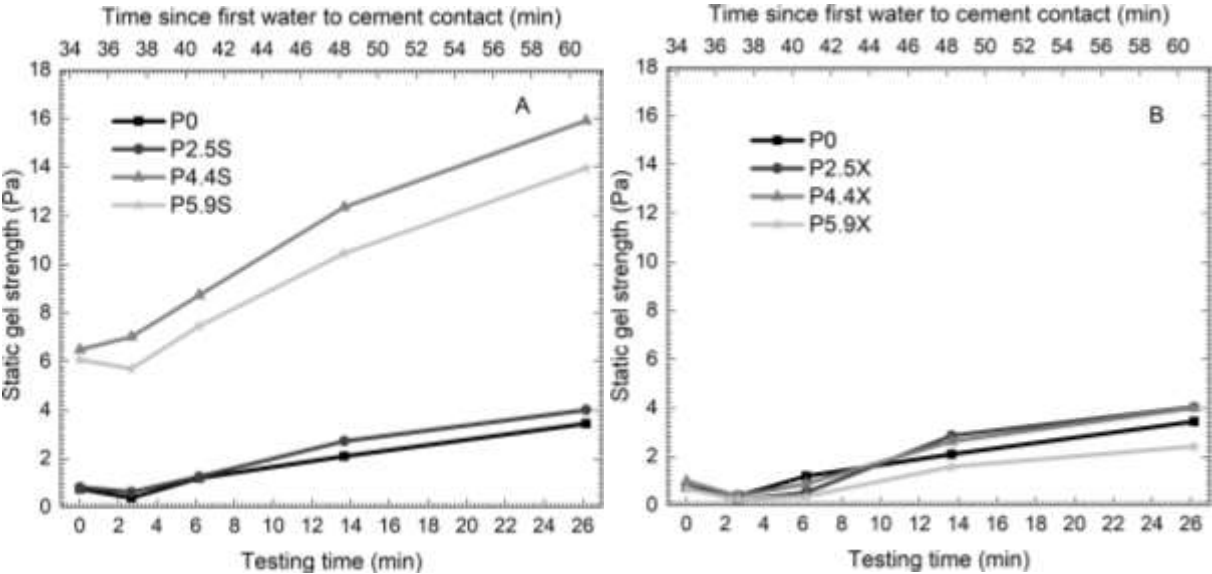

Figure 7 – Static gel strength as a function of time of A- pastes with different SBR contents and B- pastes with different XSBR contents.

The yield stress variation as a function of copolymers content and time is shown in Figure 8 A and B respectively. It can be observed that the yield stress of SBR pastes tends to increase more than that of XSBR pastes as the copolymer content increases. For example, after 26 minutes the paste containing 4.4% SBR copolymer (mid-level addition) featured a yield stress of about 30 times higher than that of the reference paste. Similar values were obtained for the paste with the highest investigated SBR copolymer addition. On the other hand, pastes with XSBR copolymer only featured a maximum yield stress of 2.1 and 1.5 times higher than that of the reference paste, at an equal testing time, respectively for mid- and highest copolymer addition levels.

Moreover, a continuous increase of the yield stress over time was observed, for both types of copolymer additions. Although a slight decrease is observed in the case of reference paste at the last testing time point. The influence of time on the yield stress of SBR pastes shows that the yield stress slightly varies in the first 6 minutes and from that point it starts to increase faster. With respect to their testing time zero, after 26 minutes, the yield stress of P5.9S and P5.9X was equal to 39.0% and 19.6%, respectively. Reference paste featured its maximum increase (20.8%) after 14 minutes, and showed a very slight decrease after 26 minutes.
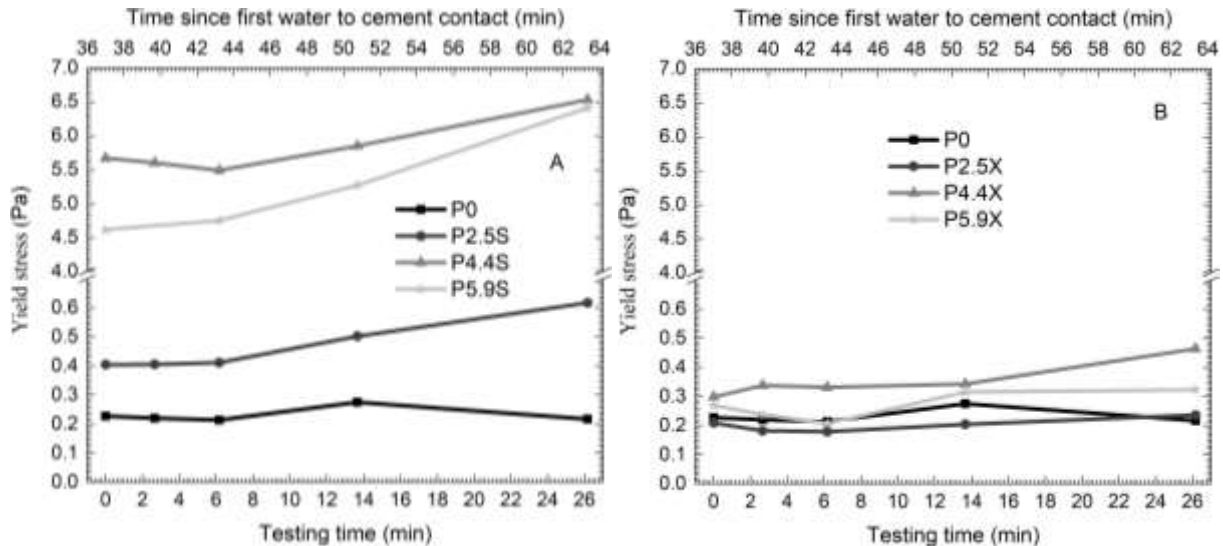
Figure 8 – Yield stress as a function of time of A- pastes with different SBR contents and B- pastes with different XSBR contents.

The changes in rheological properties of cement pastes during the induction period, besides the rheological characteristics of the existing aqueous phase, depend on the interaction of the existent solid phases with the aqueous media trapped in their pores. The aqueous phase composition depends on the solubility or water absorption capacity of the constituents of the paste, whose solid composition depends on the products formed by the hydration reactions. Thus, the opposite behavior observed for the two copolymers in their respective yield stresses can be explained as follows:

a) *The difference in polarity of SBR and XSBR*: differently to SBR, the carboxyl groups present in XSBR may result in higher absorption of water due to their polarity [44] which, in the early ages of cement may affect the effectively available free water for cement hydration reactions. The higher the XSBR content, the higher will be the presence of carboxyl groups and the higher will be the amount of absorbed water by that copolymer. Consequently, the higher the XSBR content, the lower will be the ettringite formation in the pre-induction period. On the contrary, when SBR is added to the reference cement paste there will be more water available to form ettringite in this period, compared to XSBR.

b) *The degree of new hydration product formation and respective water consumption*: the resulting liquid phase volume and paste porosity decrease as new hydration solid phases are being formed. It must be reminded that at the pre-induction period, the main hydrated phase present is the ettringite [41] which, due to its composition, consumes a significant water amount of water during its formation. As known from the literature, this formation retards the subsequent hydration reaction rates during the induction period, because its presence decreases the remaining water diffusivity during this period. This means that ettringite is not soluble in water and its formation may significantly decrease the aqueous phase volume, decreasing the plasticity of the pastes and increasing the relative solid particles volume, which in turn increases the solid phase's static resistance against any elastic strain, consequently increasing the yield stress of the paste.

14

c) *Water volume reduction and plasticizer effect of polymers:* The main factor governing the considerable increase of the yield stress value with respect to the SBR addition relies on the increased solid phase volume when the same mass of binders (high densities) were replaced by polymer (low density). The formers consist of inorganic grains, which do not interact with SBR organic long chain macromolecules. This property added to the reduced water bulk volume may reduce the solid-solid particle distances, increasing Van der Waals attractive forces and, as a consequence, the yield stress increases significantly. Oppositely, the carboxyl group XSBR may act as a plasticizer being adsorbed on the cement particle surfaces increasing the distance between grains, reducing the Van der Waals attractive forces and hindering gel network formation; Together with the lower ettringite formation, XSBR pastes have no significant impacts on the yield stress and gel strength as observed.

3.2.3 Influence of time, copolymer type and content on the plastic viscosity

Figure 9 A and B show the variation of the plastic viscosity versus time, for the pastes with different employed copolymer contents. The increase of the copolymers content also leads to an increase in the viscosity when compared to the control paste. However, with reference to this issue, each paste features its particular behavior. For the reference paste, small variations can be observed as time goes by. In the case of SBR additions, the viscosity generally tends to remain practically stable as the time increases, the highest values were measured at 14 minutes of test (with a moderate increase for the highest polymer addition). On the other hand, with the addition of XSBR latex, plastic viscosity tends to decrease as time goes by and, the greater is the copolymer addition, the higher is the decrease.
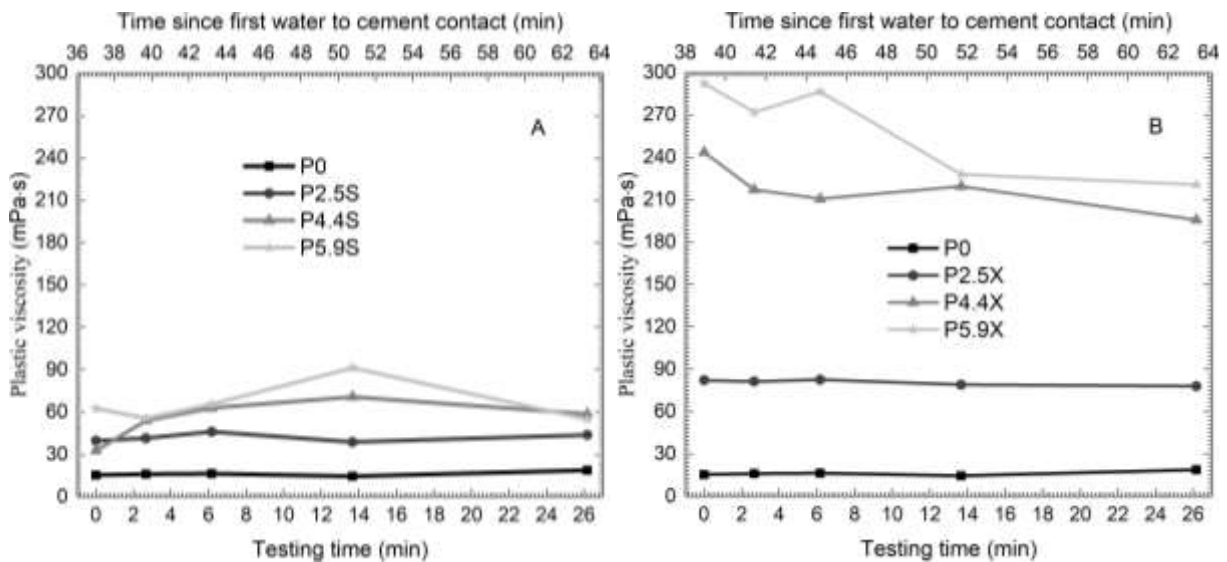

Figure 9 – Plastic viscosity as a function of time of A- pastes with different SBR contents and B- pastes with different XSBR contents.

No significant variation of respective plastic viscosity over time was observed for each paste case. This can be explained by the fact that the actual time of cement paste

15

hydration in the tests was between 30 and 65 minutes. That corresponds to the beginning of the induction period, as can be seen on the isothermal calorimetry curves (Figure 4), at which, respective ettringite phases were almost totally formed and the other reactions proceeded very slowly.

For the same reasons discussed above, the effect of the XSBR content on the increase of plastic viscosity is much more pronounced than for the same content of SBR. This also be explained due to the increase of the physical/chemical interactions between the aqueous phase and the copolymers, which are composed of long chain particles and have different water affinity as already discussed. The water absorption capacity of carboxylic groups of XSBR copolymer molecules also promotes their increase of volume. Therefore, higher physical and steric impediments occur in the presence of XSBR particles than in a paste with an equal content of SBR, which need a higher shear stress applied to have the same bulk plastic strain. In the case of XSBR copolymer, this effect is more remarkable because the carboxyl group may interact with calcium ions of the media to form complexes with twice of the initial XSBR molecule size, as can be seen in scheme of Figure 10 and reported by other researchers [12,14]. Carboxyl group may also form complexes with other cations present in the media, such as aluminum, iron and magnesium [45]. With hydrophobic characteristics, SBR increased plastic viscosity by other mechanisms, as reported elsewhere [46]. Another possible mechanism of XSBR interaction is by adsorption mechanism, where the carboxyl group facilitate molecules to envelope the cement particle surfaces [47,48]. In this case, the rise in the XSBR latex content leads to an increase in the envelope thickness that may entangle particle motion.
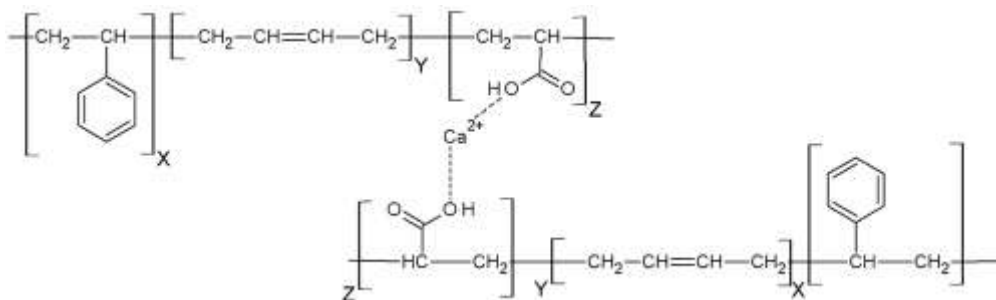

Figure 10 – Proposed mechanism of carboxyl group interaction in XSBR copolymer.

3.2.4 Influence of time, copolymer type and content on Thixotropy

The thixotropy values of the pastes with different copolymer contents versus time are shown in Figure 11 A and B. It is noticeable that there is a decrease in this parameter for all the pastes until 2.5 minutes after the test started; then, it starts increasing again. However, for P0 and XSBR pastes the thixotropic energy at all times is not higher than that at time 0, except for the paste with the lowest copolymer content after 26 minutes. On the other hand, for SBR pastes, values comparable with the initial one or slightly higher are attained after 14 minutes. Moreover, for higher SBR contents the thixotropy shows a faster increase over time. This fact indicates that, despite the first applied shear rate of 0.1 s^{-1} has been carried out for all the pastes to, theoretically, guarantee the same shear history for all the pastes, although it may have not been high enough to break out the structure at the first seconds in the case of higher SBR copolymer addition. Besides that, the paste changes in composition due to the

hydration reactions are not the same for all pastes, affecting differently the rheological properties of each paste.
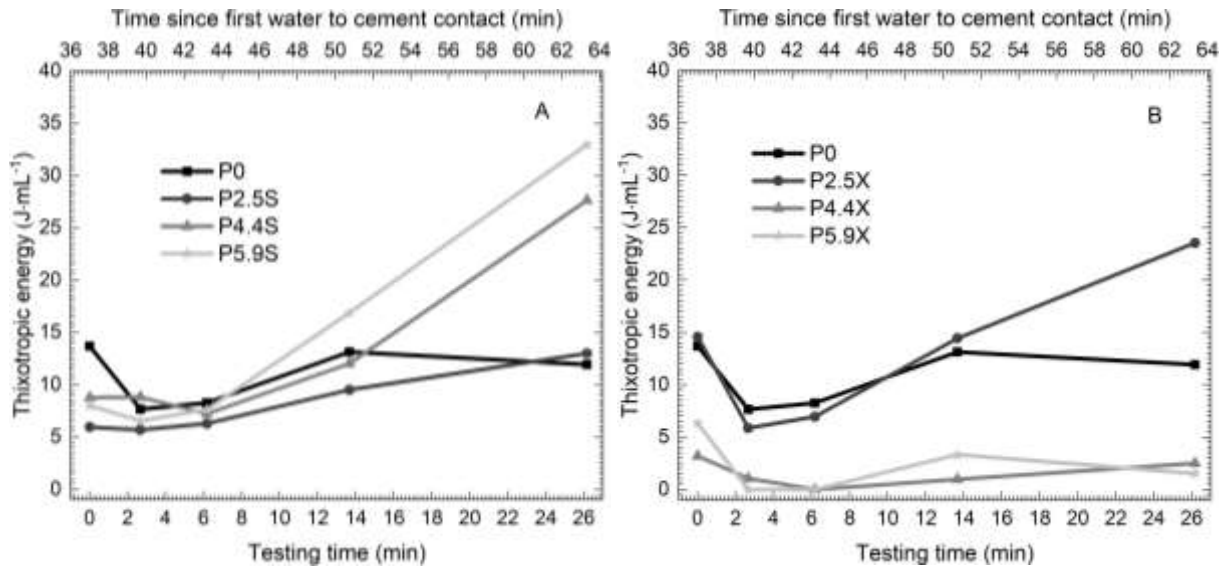

Figure 11 – Thixotropy as a function of time of A- pastes with different SBR content and B- pastes with different XSBR content.

For the investigated cement pastes, the thixotropy will depend on the changes of the hydration degree and on the respective solid and liquid constituent volume ratios, while thixotropy is being measured. Thus, as shown in Figure 11 A, SBR pastes feature higher values of the thixotropic energy than XSBR pastes. This is mainly because the latter have a lower liquid/solid phase volume ratio as a consequence of the water absorption by the XSBR copolymer. It must also be noted that the highest thixotropy values and value changes occur for the highest SBR content, because it was the case with the highest plastic viscosity and the lowest previous production of ettringite among the SBR pastes, in which case particle distribution in the dispersion can be more easily affected. Among the pastes containing XSBR, also the highest content of this copolymer causes a higher plastic viscosity, which in turn promotes the highest thixotropy.

3.3 Tracking rheological parameters by means of mini Slump test results

Figure 12 A and B show the influence of the SBR and XSBR copolymer content on the spread diameter variation as function of time for the investigated pastes. It can be observed that the increase in both copolymers content leads to reductions of the spread diameter and flow time. The decrease in the spread diameter variation reached by copolymer-modified pastes was 58% and 17% for the maximum SBR and XSBR contents respectively. The time to reach the maximum spread diameter (flow time) decreased up to the mid-level copolymer content in both cases and then increased again for their maximum content, which can be interpreted as a sort of copolymer saturation level influence. For the maximum SBR and XSBR contents, the time to reach maximum diameter were respectively 50.5% and 94% faster than that of the reference paste. This behavior, as previously explained, can be attributed to the higher viscosity

17

of these pastes, which hinders their ease to flow. This is a consequence of physical-chemical changes promoted by the copolymers presence on the cement paste first hydration stage (as previously discussed).
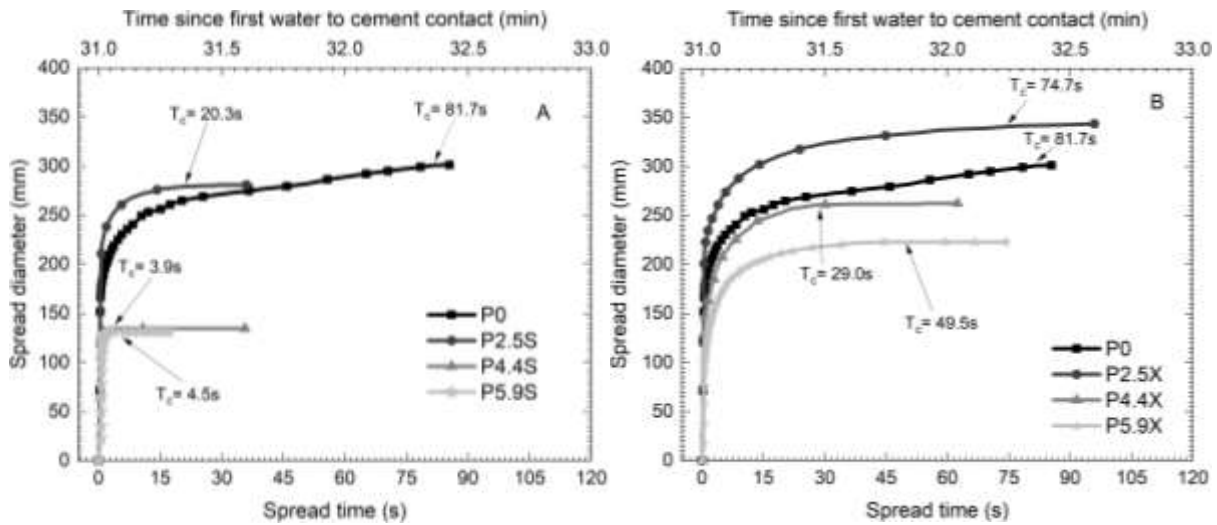

Figure 12 – Time dependent spread test properties of A- pastes with different SBR contents and B- pastes with different XSBR contents. T_c is the cutoff time of the spread velocity.

Figure 13 A and B show expanded initial details of the spread diameter variation for the pastes with different copolymer contents. As it can be observed, the initial part of the curves consists of three steps. The first step is characterized by a low spread diameter variation rate. In the second step, the spread diameter steeply increases until reaching the final step, during which the diameter variation rate decreases until flow stabilization and end. The same steps can be seen for the case of XSBR pastes.

As can be seen in Figure 13 A, the increase in the SBR content in the pastes, increases the time needed to pass from step 1 to step 2, where the pastes start to spread. In the contrast, pastes containing XSBR (Figure 13 B) feature an almost negligible increase in the time needed to reach step 2, as the copolymer content increases. This behavior can be attributed to the higher yield stress of SBR pastes as the copolymers content increase as can be observed on rheological tests seen in Figure 8 A and B. Therefore, as the gravity is the only imposed force acting on slump test, the higher is the yield stress, the higher is the time needed to surpass yield stress that keeps the bulk mass in solid-like state and put pastes to flow. This statement is also in accordance with other studies [49,50].

The passage from step 2 to step 3 represents the stage where the paste flow starts to slow down, after having reached the maximum spread rate. As can be seen from Figure 12 A the SBR addition makes the pastes to suddenly stop after having reached the maximum spread diameter. On the other hand, the addition of XSBR makes the spread rate of the pastes to reduce more gradually before reaching the maximum spread level. This behavior can also be attributed to the viscosity modifications induced by XSBR, as previously discussed.

These reductions in spread diameter, spread rate and flow time due to the increase of both the yield stress and the viscosity, as also investigated by other authors

18

[29,31] and as confirmed by rheometer test results discussed in this paper, are significantly affected by changes in the chemical reactions occurring during the hydration pre-induction and induction periods of the pastes.
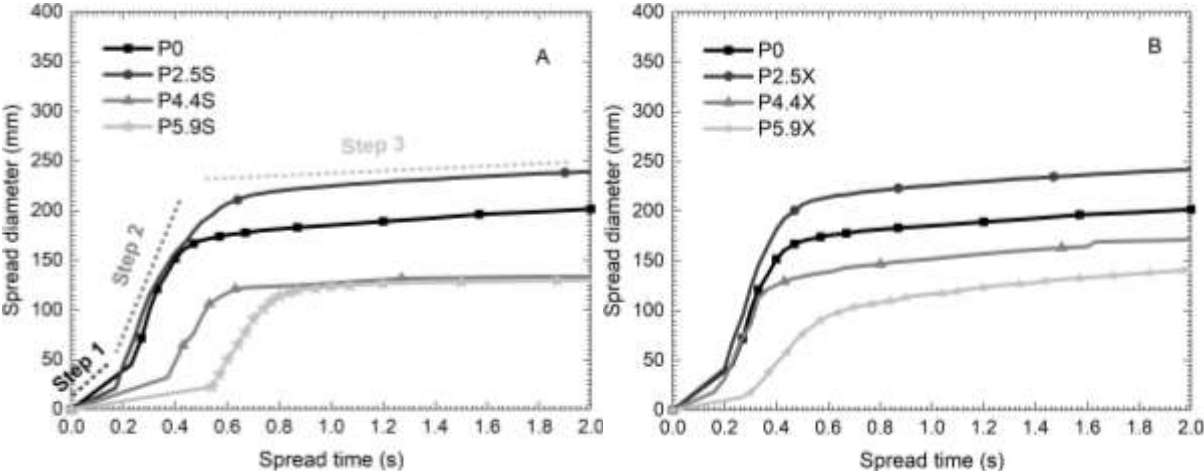

Figure 13 – Expanded graph of time dependent spread test properties of A- pastes with different SBR contents and B- pastes with different XSBR contents.

3.3.1 Identifying rheological parameters by means of instrumented spread test

Figure 14 shows the relationship between yield stress and cutoff spread diameter (D_c). It can be seen that the correlation proposed by Roussel et al. [30] is in good agreement with the experimental data, while for low spread diameter the correlation proposed by Tregger et al. [29] overestimates yield stress. An attempt to find a good correlation was done, and equation 4 was obtained with a correlation coefficient $R^2 =$ 0.97. Notice that, equation 4 is expressed also in terms of paste density (ρ_p). That is because the correlation was previously plotted in terms of τ_0/ρ versus D_c, as was also done in other studies [28–30,32,51].
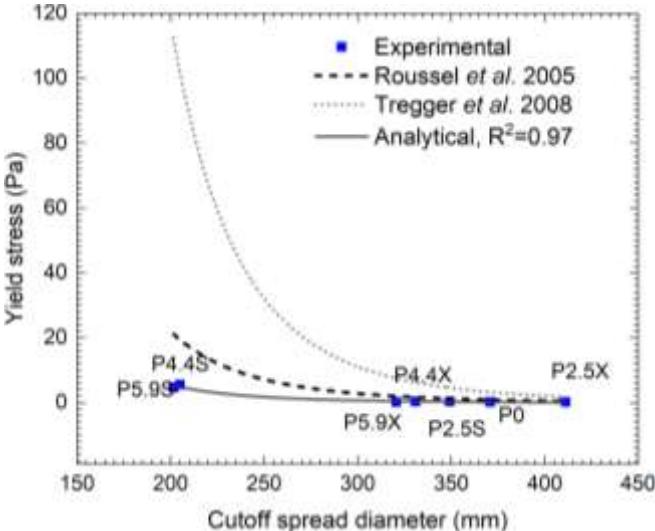

Figure 14 – Relationship between yield stress and final spread diameter.

$$\tau_0 = 2.39 \times 10^{12} \rho_p \cdot D_c^{-5.15} \qquad \text{(Equation 4)}$$

Figure 15 shows the correlation between plastic viscosity and spread properties of cement pastes. A good linear correlation was found by plotting $\mu_0/\rho_p T_c$ versus D_c, similarly to what was done in another study on concrete mixtures [32]. From the correlation, equation 5 presented a correlation coefficient of $R^2 = 0.90$. Attempts to use other research correlations were done but all failed to describe the behavior of the present cement pastes, perhaps due to the non-obvious role played by the copolymers in the rheological properties of the cement pastes, as pointed out previously, which depend on their molecular nature.
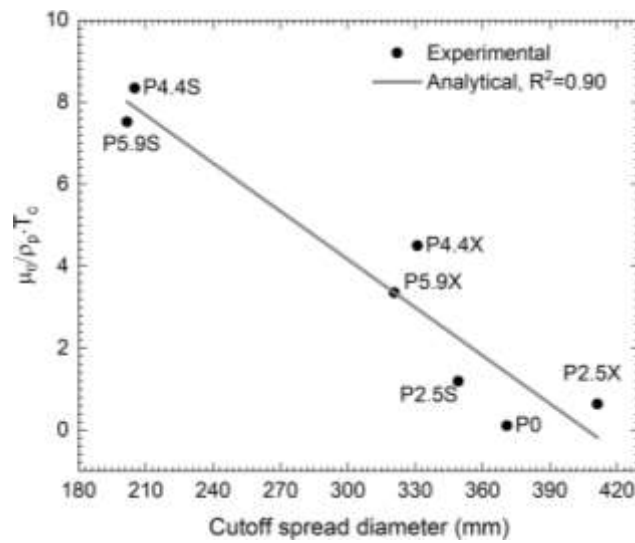

Figure 15 – Relationship between plastic viscosity with spread properties.

$$\mu_0 = -0.039\rho_p \cdot T_c \cdot (D_c - 406.54) \qquad \text{(Equation 5)}$$

4 Conclusions

- Calorimetry analysis showed to be a useful tool to track hydration kinetics and the effects of the hydration product formation on the rheological behavior of the studied pastes.
- From calorimetric data, it is possible to notice that, the opposite water affinity due to the presence or not of carboxyl group in the polymers leads to different ettringite formation in the pre-induction period. As XSBR is hydrophilic, there is less available water to form ettringite, leading to its lower formation than in SBR case.
- SBR and XSBR copolymers, despite belonging to the same class of copolymer, they affect the rheological behavior of cement pastes in a different manner due to the carboxyl group presence in the XSBR copolymer. The higher the copolymer content, the more evident are the aforementioned effects.
- The considerable higher static gel strength and yield stress found with the addition of SBR, besides promoted by having less available free water due to

the higher ettringite formation, it can be explained due to the increased solid bulk volume as a consequence of the substitution of binder particles (high density) by SBR particles (low density), which, being hydrophobic, can reduce solid particle distances increasing Van der Waals attractive forces and gel network formation.

- The carboxyl group and the water affinity of XSBR besides hindering ettringite formation may also act as a plasticizer by enveloping cement particles increasing particle distance, reducing Van der Waals attractive forces, leading to reduced static gel strength and yield stress values.

- XSBR carboxyl group may also interact with ions present in the media, leading to an increase of the plastic viscosity of the pastes due to either formation of complexes with higher particle sizes and/or to the envelopment of particles, which also lead to increased particles sizes.

- From a practical point of view, the use of these copolymers as a cement paste addition is feasible, depending on the oil well conditions. However, the peculiar features of each copolymer have to be considered. While pastes with SBR have lower plastic viscosity, XSBR, in contrast, have lower yield stress and thixotropy. This is due to the different effects that these copolymers have on the hydration products formed at pre-induction and induction periods, which occur in the fluid state.

- Remarkable correlations between field test and rheological parameters were found, which allow the use of mini-slump tests to predict yield stress and plastic viscosity indirectly by the fitted equations.

Acknowledgements

References

[1]   Nelson EB, Guillot D. Well Cementing. 2nd ed. Sugar Land, Texas, Texas: Cambridge University Press; 2006.

[2]   Suman GO, Ellis RC. World Oil's Cementing Handbook including casing handling procedures. 13th ed. Houston, Texas, USA: Gulf Publishing Company; 1977.

[3]   Eilers I. H, Root RL. Long-Term Effects of High Temperature on Strength Retrogression of Cements. 46th Annu. Calif. Reg. Meet. Soc. Pet. Eng. AIME, California, USA: Amecican Institute of Mining, Metallurgical, and Petroleum Engineers, Inc.; 1976, p. 13.

[4]   Lee H, Vimonsatit V, Chindaprasirt P, Boonserm K. Preliminary Study of Lime-Pozzolan Based Cement after Exposed to High Temperatures. Int'l J Adv Agric Environ Engg 2014;1:6–12.

[5]   Seleem HEDH, Rashad AM, Elsokary T. Effect of elevated temperature on physico-mechanical properties of blended cement concrete. Constr Build Mater 2011;25:1009–17. https://doi.org/10.1016/j.conbuildmat.2010.06.078.

[6]   Vitorino F de C. The Influence of Styrene-Butadiene and Wollastonite Fibers on Ductile Porland Cement Paste Hydration, Rheology and High Temperature Mechanical Behaviour. Universidade Federal do Rio de Janeiro, 2017.

[7]   Shin H-O, Yoo D-Y, Lee J-H, Lee S-H, Yoon Y-S. Optimized mix design for 180 MPa ultra-high-strength concrete. J Mater Res Technol 2019;8:4182–97. https://doi.org/10.1016/j.jmrt.2019.07.027.

[8]   Mosaberpanah MA, Eren O, Tarassoly AR. The effect of nano-silica and waste glass powder on mechanical, rheological, and shrinkage properties of UHPC using response surface methodology. J Mater Res Technol 2019;8:804–11. https://doi.org/10.1016/j.jmrt.2018.06.011.

[9]   DeBruijn GG, Garnier A, Brignoli R, Bexte DC, Reinheimer D. Flexible Cement Improves

Wellbore Integrity in SAGD Wells. SPE/IADC Drill. Conf. Exhib., vol. 2, Society of Petroleum Engineers; 2009, p. 1269–86. https://doi.org/10.2118/119960-MS.

[10] Correia R de F. Avaliação Mecânica e Estrutural de Pastas Cimentícias para Poços de Petróleo Submetido à Injeção de Vapor. Universidade Federal do Rio de Janeiro, 2009.

[11] Mehta PK, Monteiro PJM. Concrete: microstructure, properties, and materials. vol. 58. 3rd ed. 2006. https://doi.org/10.1036/0071462899.

[12] Ohama Y. Handbook of polymer-modified concrete and mortars. Properties and process technology. 1st ed. New Jersey: Noyes Publications; 1995.

[13] Ramalho RVA, Alves SM, Freitas JC de O, Costa BL de S, Bezerra UT. Evaluation of mechanical properties of cement slurries containing SBR latex subjected to high temperatures. J Pet Sci Eng 2019;178:787–94. https://doi.org/10.1016/j.petrol.2019.03.076.

[14] Afridi MUK, Ohama Y, Demura K, Iqbal MZ. Development of polymer films by the coalescence of polymer particles in powdered and aqueous polymer-modified mortars. Cem Concr Res 2003;33:1715–21. https://doi.org/10.1016/S0008-8846(02)01094-3.

[15] Vitorino F de C, Toledo Filho RD, Dweck J. Hydration at early ages of styrene-butadiene copolymers cementitious systems. J Therm Anal Calorim 2018;113:1041–54. https://doi.org/10.1007/s10973-017-6678-5.

[16] Taylor HFW. Cement Chemistry. 2nd ed. London, UK: Thomas Telford; 1997.

[17] Hewlett PC. Lea's Chemistry of Cement and Concrete. vol. 58. 4th ed. Elsevier Science & Technology Books; 2004.

[18] Vitorino F de C, Toledo Filho RD, Dweck J. Hydration at early ages of styrene-butadiene copolymers cementitious systems. J Therm Anal Calorim 2018;113:1041–54. https://doi.org/10.1007/s10973-017-6678-5.

[19] Kim, Yeon, Lee, Yeon. Feasibility Study of SBR-Modified Cementitious Mixtures for Use

as 3D Additive Construction Materials. Polymers (Basel) 2019;11:1321. https://doi.org/10.3390/polym11081321.

[20] Wang R, Lackner R, Wang PM. Effect of styrene-butadiene rubber latex on mechanical properties of cementitious materials highlighted by means of nanoindentation. Strain 2011;47:117–26. https://doi.org/10.1111/j.1475-1305.2008.00549.x.

[21] Sun K, Wang S, Zeng L, Peng X. Effect of styrene-butadiene rubber latex on the rheological behavior and pore structure of cement paste. Compos Part B Eng 2019;163:282–9. https://doi.org/10.1016/j.compositesb.2018.11.017.

[22] Schramm G. A Practical Approach to Rheology and Rheometry. 2nd ed. Karlsruhe, Germany: Thermo Haake; 2000.

[23] Barnes HA, Hutton JF, K. Walters FRS. An Introduction to Rheology. vol. 3. 3rd ed. Amsterdam, Netherlands: 1993.

[24] Struble LJ, Ji X. Rheology. Handb. Anal. Tech. Concr. Sci. Technol., Elsevier; 2001, p. 333–67. https://doi.org/10.1016/B978-081551437-4.50012-6.

[25] P. Ferron R, Gregori A, Sun Z, P. Shah S. Rheological Method to Evaluate Structural Buildup in Self-Consolidating Concrete Cement Pastes. ACI Mater J 2007;104:242–50.

[26] Clement C. A Scientific Approach to the Use of Thixotropic Cement. J Pet Technol 1979;31:344–6. https://doi.org/10.2118/6011-PA.

[27] Byoungsun P, Young CC. Investigating a new method to assess the self-healing performance of hardened cement pastes containing supplementary cementitious materials and crystalline admixtures. J Mater Res Technol 2019;8:6058–73. https://doi.org/10.1016/j.jmrt.2019.09.080.

[28] Ferrara L, Cremonesi M, Tregger N, Frangi A, Shah SP. On the identification of rheological properties of cement suspensions: Rheometry, Computational Fluid Dynamics modeling and field test measurements. Cem Concr Res 2012;42:1134–46.

https://doi.org/10.1016/j.cemconres.2012.05.007.

[29] Tregger N, Ferrara L, Shah SP. Identifying Viscosity of Cement Paste from Mini-Slump-Flow Test. ACI Mater J 2008;105:558–66. https://doi.org/10.14359/20197.

[30] Roussel N, Coussot P. "Fifty-cent rheometer" for yield stress measurements: From slump to spreading flow. J Rheol (N Y N Y) 2005;49:705–18. https://doi.org/10.1122/1.1879041.

[31] Roussel N, Le Roy R. The Marsh cone: A test or a rheological apparatus? Cem Concr Res 2005;35:823–30. https://doi.org/10.1016/j.cemconres.2004.08.019.

[32] Ferraris C, de Larrard F. Modified Slump Test to Measure Rheological Parameters of Fresh Concrete. Cem Concr Aggregates 1998;20:241. https://doi.org/10.1520/CCA10417J.

[33] Barghigiani TM. Caracterização Experimental de Pastas Cimentícias de Alto Desempenho Reforçadas com Fibras de Polipropileno e PVA. Universidade Federal do Rio de Janeiro - UFRJ, 2013.

[34] American Petroleum Institute. Petroleum and Gas Industries - Cements and Materials for Well Cementing - Part 1: Specification. Washington, DC, DC: 2002.

[35] Vitorino F de C. Caracterização Experimental de Pastas Cimentícias Contendo Polímero SBR em Pó e Microfibras de Volastonita. Universidade Federal do Rio de Janeiro, 2012.

[36] Benaicha M, Hafidi Alaoui A, Jalbaud O, Burtschell Y. Dosage effect of superplasticizer on self-compacting concrete: correlation between rheology and strength. J Mater Res Technol 2019;8:2063–9. https://doi.org/10.1016/j.jmrt.2019.01.015.

[37] Vitorino F de C, Toledo RDF. Rheological and Compressive Stress- Strain Behaviour under Confined and Unconfined Loads of Oilwell Cement Pastes Reinforced with Wollastonite Microfibres. Can Energy Technol Innov 2014;2:1–7.

[38]   LLC W. Admix Ampoule Accessory for use in the TAM Air Calorimeter. New Castle, DE, DE: 2011.

[39]   Bentz DP, Waller V, de Larrard F. Prediction of Adiabatic Temperature Rise in Conventional and High-Performance Concretes Using A 3-D Microstructural Model. Cem Concr Res 1998;28:285–97.

[40]   Ferraris CF, de Larrard F. Testing and Modelling of Fresh Concrete Rheology. Gaithersburg, Maryland: 1998.

[41]   Jakob C, Jansen D, Ukrainczyk N, Koenders E, Pott U, Stephan D, et al. Relating ettringite formation and rheological changes during the initial cement hydration: A comparative study applying XRD analysis, rheological measurements and modeling. Materials (Basel) 2019;12. https://doi.org/10.3390/ma12182957.

[42]   Galindo-Rosales FJ, Rubio-Hernandez FJ. Static and dynamic yield stresses of aerosil® 200 suspensionsin polypropylene glycol. Appl Rheol 2010;20:1–10. https://doi.org/10.3933/ApplRheol-20-22787.

[43]   Qian Y, Kawashima S. Use of creep recovery protocol to measure static yield stress and structural rebuilding of fresh cement pastes. Cem Concr Res 2016;90:73–9. https://doi.org/10.1016/j.cemconres.2016.09.005.

[44]   Alimardani M, Abbassi-Sourki F, Bakhshandeh GR. Preparation and characterization of carboxylated styrene butadiene rubber (XSBR)/multiwall carbon nanotubes (MWCNTs) nanocomposites. Iran Polym J (English Ed 2012;21:809–20. https://doi.org/10.1007/s13726-012-0087-1.

[45]   Wang R, Li J, Zhang T, Czarnecki L. Chemical interaction between polymer and cement in polymer-cement concrete. Bull Polish Acad Sci Tech Sci 2016;64:785–92. https://doi.org/10.1515/bpasts-2016-0087.

[46]   Yan B, Ren F, Cai M, Qiao C. Influence of new hydrophobic agent on the mechanical properties of modified cemented paste backfill. J Mater Res Technol 2019:1–12.

https://doi.org/10.1016/j.jmrt.2019.09.039.

[47] Lu Z, Kong X, Zhang C, Xing F, Cai Y, Jiang L, et al. Effect of surface modification of colloidal particles in polymer latexes on cement hydration. Constr Build Mater 2017;155:1147–57. https://doi.org/10.1016/j.conbuildmat.2017.08.114.

[48] Society R, Sciences P. Chemistry of Colloidal Silicates and Cements [and Discussion] 1983;310:67–78.

[49] de Souza Mendes PR, Thompson RL. Time-dependent yield stress materials. Curr Opin Colloid Interface Sci 2019;43:15–25. https://doi.org/10.1016/j.cocis.2019.01.018.

[50] Coussot P, Nguyen QD, Huynh HT, Bonn D. Avalanche behavior in yield stress fluids. Phys Rev Lett 2002;88:1755011–4. https://doi.org/10.1103/PhysRevLett.88.175501.

[51] de Larrard F. Concrete Mixture Proportioning - A scientific approach. 9th ed. USA and Canada, USA and Canada: Taylor & Francis e-Library; 2011.